A Mechanistic Model for Quasistatic Pulmonary Pressure-Volume Curves for Inflation

R. Amini
K. Creeden
U. Narusawa

Department of Mechanical and Industrial Engineering,
Northeastern University,
Boston, Massachusetts 02115

A mechanistic model of the respiratory system is proposed to understand differences in quasistatic pressure-volume (p-V) curves of the inflation process in terms of the alveolar recruitment and the elastic distension of the wall tissues. In the model, a total respiratory system consists of a large number of elements, each of which is a subsystem of a cylindrical chamber fitted with a piston attached to a spring. The alveolar recruitment is simulated by allowing a distribution of the critical pressure at which an element opens; while the wall distension is represented by the piston displacement. Relations are derived between parameters in the error-function p-V model equation and properties of the mechanistic model. The parameters of the model-based p-V equation are determined for clinical data sets of patients with acute respiratory distress syndrome. [DOI: 10.1115/1.1934079]

1 Introduction

Quasistatic pulmonary *p-V* (pressure-volume) curves are used routinely to obtain quantitative information on the respiratory system that is important for both research and clinical guidances, as the conditions of gas exchange are related to the characteristics of the curve. During the inflation (inspiration) and the deflation (exhalation) processes, the respiratory system changes its volume [measured in $L=(10^{-3}\ m^3)$ or mL], the lung (alveolar) pressure as well as the pleural pressure (the pressure of the thin liquid film that couples the lungs and the chest wall pleurae). The pressure p refers to the interpleural pressure difference (i.e., the difference between the lung pressure and the pleural pressure) measured in water head [cmH_2O] (1 $cmH_2O=98$ Pa). Clinical *p-V* curves are commonly obtained for an anesthetized human subject in supine position by sequentially adding (or withdrawing) incremental gas volumes (~50–100 mL) in a stepwise manner (with a duration of ~5 s per step) [1,2]. Figure 1(*a*) is a typical inflation *p-V* curve, consisting of a nearly linear region of high compliance (i.e., large dV/dp) sandwiched between two segments with low compliance at low and high pressure regions. The shape of the *p-V* curve is affected by two mechanisms, the distension of the elastic respiratory wall tissue components and the recruitment ("pop-open" mechanism) of the alveoli. The latter is the opening of the alveoli overcoming the surface tension at the interface between the gas and the liquid film lining the alveolar surfaces. A pressure increase (i.e., an increase in the interpleural pressure difference) results in the recruitment of a greater number of alveoli. The high compliance is believed to be associated with both the distension of open parts of the lungs and the (alveolar) recruitment of collapsed parts of the lungs [3]. Some protective ventilation strategies, based on patients' quasistatic *p-V* curves, have been proposed for lung disease patients in intensive care units. Amato and coworkers [4,5] demonstrated, based on their clinical study involving patients with acute respiratory distress syndrome (ARDS), that a ventilator strategy guided by the *p-V* curve resulted in reduced lung trauma, a high weaning rate, and improved survival compared with a conventional ventilator strategy without the *p-V* curve guidance. Also, a recent ARDS Network report [6] on a clinical study involving 861 patients shows lower mortality in the group treated with lower tidal volumes than in the group treated with traditional higher tidal volumes. Although a use of *p-V* curves is not mentioned, the report underscores the importance of optimized ventilator strategy.

In order to quantify the characteristics of *p-V* curves as well as their changes observed in clinical settings, various *p-V* model equations have been proposed [7–12]. Parameters in model equations are determined from statistical processing of clinical data. It is important that these parameters should have some physiological interpretations. Also, to understand the shape of *p-V* curves in terms of mechanical behavior of lungs, multicompartment lung models were developed and used to obtain information on the effects of lung elasticity and a degree of alveolar recruitment on *p-V* curves [3,13]. Although these analyses serve to relate the internal elastic conditions of the total respiratory system (TRS) to general *p-V* curve behavior, there has been no attempt to interpret individual differences in *p-V* curves directly in terms of internal elastic properties, alveolar recruitment, and their changes. From an analytical viewpoint, the quasistatic *p-V* curves are more amenable to theoretical studies because at each state we may be able to apply equilibrium principles. An overall objective of this report is to test the hypothesis that a mechanistic model, based on the continuous alveolar recruitment and the elastic distension of the wall tissues, is effective in understanding a relation between the observed TRS conditions (as *p-V* curves) and the corresponding internal respiratory response (in terms of the mechanistic model) during the inflation process.

2 Continuous Equation for Quasistatic *p-V* Curves

In the past, the high compliance midregion and the low compliance low- and high-pressure regions along the *p-V* curve are repesented by three separate equations for quantitative analyses. Typically the midregion is approximated by a linear *p-V* equation; while, the low compliance low- and high-pressure regions are expressed by exponential equations. A term, the lower (upper) inflection point [LIP (UIP)], refers to the pressure location where the linear midregion equation meets the nonlinear, low- (high-) pressure regions. The compliance of the linear midregion (chord

Contributed by the Bioengineering Division for publication in the JOURNAL OF BIOMECHANICAL ENGINEERING. Manuscript received April 21, 2004; revision received February 22, 2005. Associate Editor: Fumihiko Kajiya.

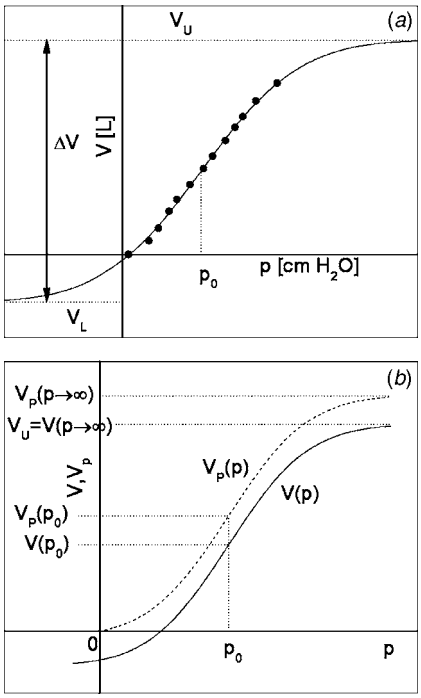

Fig. 1 (*a*) A typical quasistatic pulmonary pressure-volume curve, (*b*) *V*(*p*) vs $V_p(p)$

compliance), LIP and UIP are the most commonly used parameters to quantify *p-V* curve characteristics in the analyses based on the piecewise continuous *p-V* model equation.

More recently two continuous *p-V* model equations are proposed that simulate various *p-V* curves accurately over the entire range of *p-V* data. One is a sigmoidal (tangent hyperbolic) equation, and the other an error-function equation, both originally proposed by Venegas and his coworkers [1]. The error function *p-V* equation may be expressed as

$$\frac{dV}{dp}=\frac{\alpha}{4}(\Delta V)^2\exp\left[-\left(\frac{\sqrt{\pi}}{4}\Lambda\right)^2\left(\frac{p}{p_0}-1\right)^2\right], \tag{1a}$$

$$V=V_U-\frac{\Delta V}{2}+\left(\frac{\Delta V}{2}\right)\mathrm{erf}\left(\frac{\sqrt{\pi}}{4}\Lambda\left(\frac{p}{p_0}-1\right)\right), \tag{1b}$$

where $\Delta V=V_U-V_L$, V_U=the upper asymptote, V_L=the lower asymptote, α=positive constant, Λ (nondimensional)$=\alpha p_0\Delta V$, and p_0=a pressure at the midpoint (inflection point) of the curve [1,2,14]

$$\mathrm{erf}(x)=\frac{2}{\sqrt{\pi}}\int_0^x e^{-t^2}dt \quad \mathrm{erf}(\infty)=1, \quad \mathrm{erf}(-x)=-\mathrm{erf}(x).$$

The sigmoidal (tangent hyperbolic) *p-V* equation is

$$\frac{dV}{dp}=-\alpha(V-V_U)(V-V_L), \tag{1c}$$

$$\frac{V-V_L}{\Delta V}=\{1+\exp[-\alpha\Delta V(p-p_0)]\}^{-1}. \tag{1d}$$

The *p-V* curve plotted in Fig. 1(*a*) may represent either Eq. (1*b*) or Eq. (1*d*). The corresponding nondimensional forms are

For the error function *p-V* equation

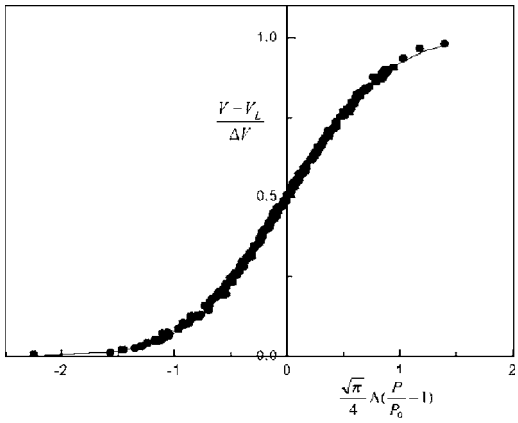

Fig. 2 Error-function *p-V* equation and inflation data points

$$\frac{d\bar{V}}{d\bar{p}}=\frac{\Lambda}{2}\cdot\exp\left(-\frac{\pi}{4}\omega^2\right), \quad \bar{V}=\mathrm{erf}\left(\frac{\sqrt{\pi}}{2}\omega\right). \tag{2a}$$

For the sigmoidal (tangent hyperbolic) *p-V* equation

$$\frac{d\bar{V}}{d\bar{p}}=\frac{\Lambda}{2}(1-\bar{V}^2), \quad \bar{V}=\tanh(\omega)\left(=\frac{e^{\omega}-e^{-\omega}}{e^{\omega}+e^{-\omega}}\right), \tag{2b}$$

where $\bar{V}=[V-(V_U+V_L)/2]/(\Delta V/2)$, $\bar{p}=(p/p_0)-1$, $\omega=\Lambda\bar{p}/2$.

Equation (2) satisfies the following conditions:

$$\bar{V}(\bar{p}=0)=0,$$

$$\bar{V}(\bar{p})=-\bar{V}(-\bar{p}) \text{ (antisymmetry with respect to } p=p_0),$$

$$d\bar{V}/d\bar{p}(\bar{p}=0)=\Lambda/2, \quad \bar{V}(\bar{p}\to\pm\infty)=\pm1, \quad d\bar{V}(\bar{p}\to\pm\infty)/d\bar{p}=0.$$

A clinical data source of *p-V* curves we use in the present analyses are 21 data sets of ARDS patients (both inflation and deflation data) in supine position by Harris et al. [2]. Data sets are analyzed by minimizing the difference between data points and the error function model equation through the application of the method of least squares to obtain the parameters Λ, ΔV, p_0 and V_U (or V_L). Plotted in Fig. 2 are 264 inflation data points in terms of Eq. (1*b*), $(V-V_L)/\Delta V$ versus $\sqrt{\pi}\Lambda(p/p_0-1)/4$. Agreement is excellent between the data and the *p-V* equation with R^2 (the coefficient of determination) =0.999 38. The deflation process (225 data points) is also confirmed to fit well with the *p-V* equation (R^2 =0.999 07). One of the motivations of the present study is that the accuracy with which the continuous *p-V* model equations simulate *p-V* curves may imply its physical significance as a signature of the state within TRS.

3 Development of a Mechanistic Model

A TRS consists of a large population of basic elements (N =total number of elements) with a distribution parameter, p_{cj} defined as

p_{cj} = a critical pressure at which an element j pops open,

representing the alveolar recruitment.

The distribution of elements over p_{cj} reflects an observation expressed by many investigators that the alveolar recruitment occurs gradually along a *p-V* curve. Referring to Fig. 3, an arbitrary element j consists of a cylindrical chamber with a piston-spring system (A_s=piston surface area, k=spring constant [N/m],

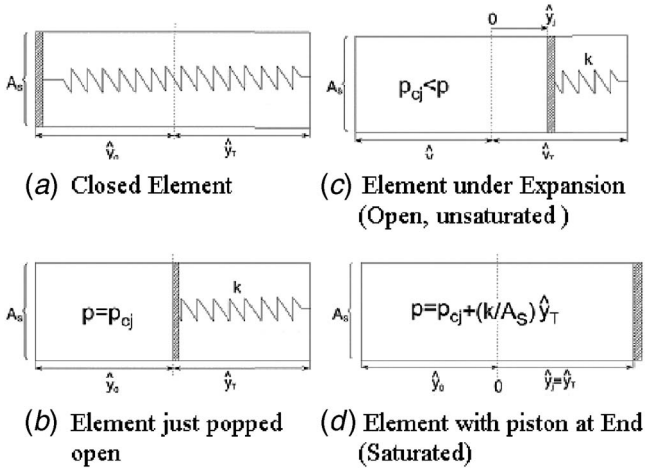

Fig. 3 A schematic diagram of mechanistic model of TRS element

$\hat{y}_0$=piston displacement due to pop-open mechanism, $\hat{y}_T$=piston displacement due to elastic wall distension). The element is closed when the piston is located at the left end of the cylinder as shown in Fig. 3(*a*). When pressure acting on the left-hand side of the piston reaches p_{cj}, the piston suddenly moves to a new position ("pop-open" mechanism=the recruitment of alveoli) with $\hat{V}_0(=A_s \cdot \hat{y}_0)$ indicating an elemental volume increase due to the piston displacement of $\hat{y}_0$ [Fig. 3(*b*)]. Any further increase in pressure results in a volume increase as the piston moves to the right [Fig. 3(*c*)] until it reaches the end of the cylinder [Fig. 3(*d*)]. (The symbol "^" indicates an elemental quantity.) The elemental volume $\hat{V}_j$ at p ($\geqslant p_{cj}$) is equal to $\hat{V}_0+A_s\hat{y}_j$; which, upon an application of a quasistatic force balance across the piston, $A_s(p-p_{cj})=k\hat{y}_j$, becomes

$$\hat{V}_j = \hat{V}_0 + (A_s^2/k)(p - p_{cj}),$$

relating the elemental volume change to the pressure increase above the critical pop-open pressure. Also by setting $\hat{V}_j=A_s(\hat{y}_0+\hat{y}_T)$ in the equation written above, the piston position of an element reaches its stroke limit of $\hat{y}_T$ when pressure p reaches

$$(p_{cj} + (k/A_s)\hat{y}_T).$$

The mechanistic model of an element, therefore, goes through three stages in the inflation process—closed, open, and unsaturated (i.e., $\hat{y}_j<\hat{y}_T$) and open and saturated (i.e., $\hat{y}_j=\hat{y}_T$). The model assumes that such properties of the basic element as k, A_s, $\hat{V}_0$, and $\hat{y}_T$ are constant and common to all elements. The energy level of an open and unsaturated element j consists of the activation energy required to pop open the element $\hat{\epsilon}_{jA}$ and the energy stored in the spring $\hat{\epsilon}_{jS}$. For $\hat{\epsilon}_{jA}$, we assign the compression/expansion work under constant pressure; i.e., $\hat{\epsilon}_{jA}=p_{cj}\hat{V}_0$; while, $\hat{\epsilon}_{jS}$ is equal to $k\hat{y}_j^2/2$, which may be expressed in terms of p_{cj} as $\hat{\epsilon}_{jS}=(A_s^2/2k)(p-p_{cj})^2$ from an application of the force balance. In summary, at a quasistatic (quasiequilibrium) state at $p=p$, an open TRS element j with its critical pop-open pressure p_{cj} belongs to one of the following conditions:

- For $p_{cj}=p$, the element j pops open with $\hat{V}_j=\hat{V}_0$, $\hat{\epsilon}_j=p_{cj}\hat{V}_0$.
- For $p-(k/A_s)\hat{y}_T<p_{cj}<p$, the piston of the open and unsaturated element j moves to a location $\hat{y}_j$ with $\hat{V}_j=\hat{V}_0+A_s\hat{y}_j$ $\hat{\epsilon}_j=p_{cj}\hat{V}_0+(A_s^2/2k)(p-p_{cj})^2$.
- For $p_{cj}\leqslant p-(k/A_s)\hat{y}_T$, the piston of the open and saturated element j remains at the stroke limit $\hat{y}_T$ with $\hat{V}_j=\hat{V}_0+A_s\hat{y}_T$, $\hat{\epsilon}_j=p_{cj}\hat{V}_0+(k/2)\hat{y}_T^2$.

The state of an element follows the sequence above during the inflation process as p increases. To obtain an explicit form of the distribution function of TRS elements over the distribution parameter p_{cj}, we focus on open and unsaturated elements, for which the elemental energy shown above may be rewritten as

$$\hat{\epsilon}_j(\text{open,unsaturated}) = \frac{A_s^2}{2k}\left[p_{cj} - \left(p - \frac{k\hat{V}_0}{A_s^2}\right)\right]^2 + \frac{\hat{V}_0}{2}\left(2p - \frac{k\hat{V}_0}{A_s^2}\right). \tag{3}$$

According to the Boltzmann statistical model ([15,16] for example), which assumes that there is no limit in the number of elements per energy state, the most probable distribution N_j/N (a number fraction of elements at an energy level, $\hat{\epsilon}_j$), may be expressed as

$$N_j/N = e^{-\beta\hat{\epsilon}_j} \Big/ \sum_j e^{-\beta\hat{\epsilon}_j} \quad (\beta = \text{unspecified constant}) \tag{4}$$

where N_j is the number of elements at energy level j and N is the total number of TRS elements.

A substitution of Eq. (3) into Eq. (4) with the summation replaced by an integral over the whole range of p_{cj} for a large number of elements, yields

$$\frac{dN_j}{Ndp_{cj}} = \exp\left(-\frac{\hat{\beta}}{2}\left(p - p_{cj} - \frac{k}{A_s^2}\hat{V}_0\right)^2\right) \Big/ \int_{-\infty}^{\infty} \exp\left(-\frac{\hat{\beta}}{2}\left(p - p_{cj} - \frac{k}{A_s^2}\hat{V}_0\right)^2\right) dp_{cj}, \tag{5}$$

where $\hat{\beta}$ is the $(A_s^2/k)\beta$ The second term of Eq. (3), upon substitution to Eq. (4), drops out as a common factor. It should also be noted that the integration with respect to p_{cj} in the denominator ranges from $-\infty$ and $+\infty$. As summarized above, any arbitrary element remains active (open and unsaturated) only in a certain range of p_{cj}; therefore, the application of Eq. (5) over the entire range of $-\infty<p_{cj}<\infty$ assumes that the distribution function that is valid for active elements is also applicable in evaluating the number of closed as well as saturated elements. Then, upon performing the integration of the denominator in Eq. (5), we obtain for dN_j/N (= a number fraction of elements, for which the magnitude of p_{cj} ranges between p_{cj} and $p_{cj}+dp_{cj}$)

$$\frac{dN_j}{N} = f \cdot dp_{cj}, \quad f = \left(\frac{\hat{\beta}}{2\pi}\right)^{1/2} \exp\left[-\frac{\hat{\beta}}{2}\left(p - p_{cj} - \frac{k}{A_s^2}\hat{V}_0\right)^2\right]. \tag{6}$$

Noting that elements, j, with p_{cj} in the range of $0\leqslant p_{cj}\leqslant p$, are open at $p=p$, and that $(k/A_s)\hat{y}_T(\equiv B)$ is the pressure at which an element j with $p_{cj}=0$ reaches the piston stroke limit of $\hat{y}_T$, the

volume change needs to be evaluated for the following two pressure ranges: Pressure range 1:$0 \leqslant p \leqslant B$ and pressure range 2: $B \leqslant p$.

3.1 Pressure Range 1: $0 \leqslant p < B$. Since the pressure is below B (the threshold pressure for the onset of saturation), all open elements are active (unsaturated) with $\hat{y}_j < \hat{y}_T$. Then an overall volume change of TRS, $V_p(p)$, from the state of $p=0$ is

$$V_p(p) = N\left[\int_{p_{cj}=0}^{p} (\hat{V}_0 + A_s\hat{y}_j) f(p=p)dp_{cj} + \int_{p_{cj}=p}^{\infty} A_s\hat{y}_j f(p=p)dp_{cj}\right]. \tag{7a}$$

The first term on the right-hand side represents a volume increase due to the elements that popped open at $p=p_{cj}$, followed by a piston displacement $\hat{y}_j$ [$=A_s(p-p_{cj})/k$ from the force balance] during the inflation process from $p=0$ to $p=p$. The second term results from the following observations: At $p=p$, elements in the range of $0 \leqslant p_{cj} \leqslant p$ are recruited by the alveolar pop-open mechanism. Since the distribution function, f of Eq. (6) shifts to the right with an increase in p on the p_{cj} versus the f diagram, the number of open elements increases with pressure. Also the following relation holds true

$$\int_{p_{cj}=p}^{\infty} f(p=p)dp_{cj} = \int_{p_{cj}=0}^{\infty} f(p=0)dp_{cj}. \tag{7b}$$

The equation above maintains that the number fraction of elements with their critical pop-open pressure p_{cj} being greater than p is constant and independent of the magnitude of p. Since the region of $p_{cj} \geqslant 0$ in the distribution function represents the elements that are actively involved in the volume change, the right-hand side of the equation above corresponds to the number fraction of elements that are active at $p=0$. Hence, the second term of Eq. (7*a*) is interpreted as the volume change of elements that are already open at $p=0$ (nonalveolar elements). For these elements the piston displacement $\hat{y}_j (=A_s p/k)$ is the only mechanism available for the volume change during the inflation process.

Then, after expressing $\hat{y}_j$ in terms of p and p_{cj}, Eq. (7*a*) may be written as

$$V_p = N\left(\frac{\hat{\beta}}{2\pi}\right)^{1/2}\left[\int_{-A}^{p-A}\left(2\hat{V}_0 + \frac{A_s^2}{k}t\right)\exp\left(-\frac{\hat{\beta}}{2}t^2\right)dt + \int_{A}^{\infty}\frac{A_s^2}{k}\cdot p\cdot\exp\left(-\frac{\hat{\beta}}{2}z^2\right)dz\right], \tag{7}$$

where $A=(k/A_s)\hat{y}_0$, $t=-z=(p-p_{cj}-k\hat{V}_0/A_s^2)$. It is noted that the definition of $V_p(p=0)=0$ is satisfied by Eq. (7).

3.2 Pressure Range 2: $B \leqslant p$. In this pressure range, elements with $0 \leqslant p_{cj} \leqslant p-B$ as well as elements that are already open at $p=0$ are saturated (i.e., $\hat{y}_j = \hat{y}_T$ for the elements); while, elements with $p-B \leqslant p_{cj} \leqslant p$ remain unsaturated (i.e., $\hat{y}_j < \hat{y}_T$); therefore

$$V_p = N\int_0^{p-B}(\hat{V}_0 + A_s\hat{y}_T)f(p=p)dp_{cj} + N\int_{p-B}^{p}(\hat{V}_0 + A_s\hat{y}_j)\cdot f(p=p)dp_{cj} + N\int_p^{\infty} A_s\hat{y}_T\cdot f(p=p)dp_{cj}. \tag{8}$$

Equations (7) and (8), after integration, become

$$V_p(0 \leqslant p \leqslant B) = N\hat{V}_0\left[I_1 + \frac{1}{2}\frac{p}{A}(1-I_1) - \frac{I_2(p)}{2\sqrt{\pi}C} + I_3(p)\right], \tag{9a}$$

$$V_p(B \leqslant p) = N\hat{V}_0\left[I_1 + \frac{\hat{y}_{T0}}{2}(1-I_1) + \frac{\hat{y}_{T0}-1}{2}I_4 - \frac{I_5}{2\sqrt{\pi}C} + \frac{\hat{y}_{T0}+1}{2}I_3(p)\right], \tag{9b}$$

where

$$I_1 = \mathrm{erf}(C), \quad I_2(p) = \exp\left[-C^2\left(\frac{p}{A}-1\right)^2\right] - \exp(-C^2),$$

$$I_3(p) = \mathrm{erf}\left[C\left(\frac{p}{A}-1\right)\right],$$

$$I_4 = \mathrm{erf}[C(1-\hat{y}_{T0})], \quad I_5 = \exp[-C^2(\hat{y}_{T0}-1)^2] - \exp(-C^2),$$

$$C = (\hat{\beta}/2)^{1/2}\cdot A, \quad \hat{y}_{T0} = \hat{y}_T/\hat{y}_0 = B/A.$$

A measured volume V is generally not exactly zero at $p=0$; while, by definition, V_p is zero at $p=0$. Referring to Fig. 1(*b*), the relation between $V(p)$ and $V_p(p)$ is

$$V_p(p\to\infty) - V_U = V_p(p=p) - V(p=p);$$

hence, the mechanistic model yields the following p-V equation:

$$V(0 \leqslant p \leqslant B) = V_U + N\hat{V}_0\left(\frac{(1-I_1)}{2}\left(\frac{p}{A} - \hat{y}_{T0}\right) - \frac{\hat{y}_{T0}+1}{2} - \frac{\hat{y}_{T0}-1}{2}\cdot I_4 + \frac{I_5 - I_2(p)}{2\sqrt{\pi}C} + I_3(p)\right), \tag{10a}$$

$$V(B \leqslant p) = V_U - \frac{N\hat{V}_0(\hat{y}_{T0}+1)}{2} + \frac{N\hat{V}_0(\hat{y}_{T0}+1)}{2}\cdot I_3(p). \tag{10b}$$

In order to relate the mechanistic model, to the p-V curve, an additional condition that needs to be satisfied is conservation of energy. For a quasistatic process from an initial state of $[p=0, V=V(p=0)]$ to a final state of $[p=p_f, V=V(p=p_f)]$ (p_f=the pressure at the end of a measured p-V curve), the conservation of energy may be written as

$$\Delta U[\equiv U(p=p_f) - U(p=0)] = \int_{V(p=0)}^{V(p=p_f)} p dV, \tag{11}$$

where $U(p=p_f)$ represents the total energy of TRS at $p=p_f$ to be evaluated from our mechanistic model; while the right-hand side of the equation is work associated with the inflation process that must be evaluated from the p-V model equation.

4 Mechanistic Model versus Error Function p-V Equation

Relations between the parameters in the error function p-V equation and the parameters in our mechanistic model are derived based on the observation that the p-V relation Eq. (10*b*) for the high pressure region as well as the corresponding equation for the local compliance,

$$\frac{dV}{dp}(B \leqslant p) = \frac{N\hat{V}_0(\hat{y}_{T0}+1)}{2}\cdot\frac{2C}{\sqrt{\pi}p_0}\cdot\exp\left(-C^2\left(\frac{p}{A}-1\right)^2\right),$$

become identical to the error function model equation, Eqs. (1*a*) and (1*b*), if we set

$$N\hat{V}_0(\hat{y}_{T0}+1)=\Delta V,\quad A(\equiv(k/A_s)\hat{y}_0)=p_0,$$
$$C\left(\equiv\left(\frac{\hat{\beta}}{2}\right)^{1/2}\cdot A\right)=\frac{\sqrt{\pi}}{4}\Lambda. \tag{12}$$

Before further developments are made on the mechanistic model, our results are summarized below, based on the parametric relations Eq. (12) between the error function p-V equation and the model.

4.1 Pressure-Volume (p-V_p) equation.

$$V_p(0\leqslant p\leqslant p_0\cdot\hat{y}_{T0})=\frac{\Delta V}{\hat{y}_{T0}+1}\left(I_1+\frac{(\bar{p}+1)(1-I_1)}{2}-\frac{2I_2(\bar{p})}{\pi\Lambda}+I_3(\bar{p})\right),$$

$$V_p(p_0\cdot\hat{y}_{T0}\leqslant p)=\frac{\Delta V}{\hat{y}_{T0}+1}\left(I_1+\frac{\hat{y}_{T0}}{2}(1-I_1)+\frac{\hat{y}_{T0}-1}{2}I_4-\frac{2I_5}{\pi\Lambda}+\frac{\hat{y}_{T0}+1}{2}\cdot I_3(\bar{p})\right). \tag{13a}$$

4.2 Pressure-Volume (p-V) equation.

$$V(0\leqslant p\leqslant p_0\cdot\hat{y}_{T0})=\frac{V_U+V_L}{2}+\frac{\Delta V}{\hat{y}_{T0}+1}\left(I_3(\bar{p})+\frac{(1-I_1)}{2}\cdot(\bar{p}+1-\hat{y}_{T0})-\frac{\hat{y}_{T0}-1}{2}I_4+\frac{2(I_5-I_2(\bar{p}))}{\pi\Lambda}\right),$$

$$V(p_0\cdot\hat{y}_{T0}\leqslant p)=\frac{V_U+V_L}{2}+\frac{\Delta V}{2}I_3(\bar{p}) \tag{13b}$$

where

$$I_1=\mathrm{erf}(C),\quad I_2(\bar{p})=\exp(-C^2\bar{p}^2)-\exp(-C^2),$$
$$I_3(\bar{p})=\mathrm{erf}(C\bar{p}),$$
$$I_4=\mathrm{erf}(C(1-\hat{y}_{T0})),\quad I_5=\exp[-C^2(\hat{y}_{T0}-1)^2]-\exp(-C^2),$$
$$C=\sqrt{\pi}\Lambda/4.$$

4.3 Distribution function.

$$\frac{dN_j}{N\cdot dp_{cj}}=f(p),\quad f(p)=\frac{1}{\sqrt{2\pi}\sigma_D}\cdot\exp\left(-\frac{1}{2}\left[\frac{p_{cj}-(p-p_0)}{\sigma_D}\right]^2\right) \tag{13c}$$

or in normalized form,

$$\frac{dN_j}{N\cdot d\hat{p}_{cj}}=F(\bar{p}),\quad F(\bar{p})=\frac{1}{\sqrt{2\pi}\sigma}\cdot\exp\left(-\frac{1}{2}\left[\frac{\hat{p}_{cj}-\bar{p}}{\sigma}\right]^2\right),$$

where

$$\hat{p}_{cj}=p_{cj}/p_0,\quad \sigma=(8/\pi)^{1/2}/\Lambda(\approx 1.596/\Lambda),\quad \sigma_D=p_0\sigma. \tag{13d}$$

The p-V equation for the lower pressure region as well as the boundary pressure between the high- and low-pressure regions contain the parameters of the p-V equation Λ, p_0, ΔV, V_U (*or* V_L), and an additional parameter $\hat{y}_{T0}$ of the mechanistic model. Conservation of energy Eq. (11) is utilized to find the magnitude of $\hat{y}_{T0}$. Similar to the p-V model equation Eq. (13*b*) the evaluation of Eq. (11) depends on the magnitude of the final pressure p_f relative to the boundary pressure $p_0\hat{y}_{T0}$ between the high- and low-pressure regions. As will be shown later in the analyses of clinical data, the magnitude of $\hat{y}_{T0}$ is less than unity; hence, the conservation of energy is further developed for the case of $p_0\cdot\hat{y}_{T0}\leqslant p_f$ [i.e., $\hat{y}_{T0}-1\leqslant\bar{p}_f(=p_f/p_0-1)$] The left-hand side of Eq. (11) may be evaluated from the elemental distribution function, $F(\bar{p})$ of Eq. (13*c*), along with the elemental energy summarized in the paragraphs preceding Eq. (3), yielding

$$\Delta U=\frac{Np_0^2A_s^2}{k}\left[\int_0^{\bar{p}_f+1-\hat{y}_{T0}}\left(\hat{p}_{cj}+\frac{1}{2}\hat{y}_{T0}^2\right)\cdot F(\bar{p}=\bar{p}_f)d\hat{p}_{cj}+\int_{\bar{p}_f+1-\hat{y}_{T0}}^{\bar{p}_f+1}\left(\hat{p}_{cj}+\frac{1}{2}(\bar{p}_f+1-\hat{p}_{cj})^2\right)\cdot F(\bar{p}=\bar{p}_f)d\hat{p}_{cj}+\int_{\bar{p}_f+1}^{\infty}\frac{1}{2}\hat{y}_{T0}^2\cdot F(\bar{p}=\bar{p}_f)d\hat{p}_{cj}\right]=\frac{Np_0^2A_s^2}{k}\left[-\frac{2}{\pi\Lambda}[I_5-I_2(\bar{p}_f)]+\frac{1}{4}\hat{y}_{T0}^2[I_3(\bar{p}_f)+I_4]+\frac{1}{2}\bar{p}_f[I_1+I_3(\bar{p}_f)]+\frac{1}{4}(I_1-I_4)+\frac{2}{\pi\Lambda}\left(\frac{1}{\Lambda}(I_1-I_4)-\frac{1}{2}[(\exp(-C^2)-(1-\hat{y}_{T0})\cdot\exp(-C^2(1-\hat{y}_{T0})^2)\ ]\right)+\frac{\hat{y}_{T0}^2}{4}(1-I_1)\right]. \tag{14a}$$

The right-hand side of Eq. (11) becomes

$$\int_{V(p=0)}^{V(p=p_f)}pdV=p_fV(p=p_f)-\left[\int_0^{p_0\hat{y}_{T0}}V(0\leqslant p\leqslant p_0\hat{y}_{T0})dp+\int_{p_0\hat{y}_{T0}}^{p_f}V(p_0\hat{y}_{T0}\leqslant p_f)dp\right]$$
$$=\frac{p_0\Delta V}{\hat{y}_{T0}+1}\left[\frac{(\hat{y}_{T0}+1)}{2}(\bar{p}_f+1)I_3(\bar{p}_f)+\frac{\hat{y}_{T0}(\hat{y}_{T0}-1)}{2}\cdot I_4-\frac{2}{\pi\Lambda}\hat{y}_{T0}\cdot I_5-\int_{-1}^{\hat{y}_{T0}-1}I_3(\bar{p})d\bar{p}+\frac{4}{\pi\Lambda^2}(I_1-I_4)-\frac{2}{\pi\Lambda}\hat{y}_{T0}\cdot\exp(-C^2)-\frac{\hat{y}_{T0}+1}{2}\int_{\hat{y}_{T0}-1}^{\bar{p}_f}I_3(\bar{p})d\bar{p}+\frac{\hat{y}_{T0}^2}{4}(1-I_1)\right]. \tag{14b}$$

It should be noted that the factors $Np_0^2A_s^2/k$ in Eq. (14*a*) and $p_0\Delta V/(\hat{y}_{T0}+1)$, in Eq. (14*b*) are identical, thus dropping out of the conservation of energy Eq. (11) as the common factor.

The p-V equation constructed from the mechanistic model Eq. (13*b*) contains five unknowns [Λ, p_0, ΔV, V_U (*or* V_L), $\hat{y}_{T0}$], the magnitudes of which are determined by minimizing the differences between Eq. (13*b*) and a specified data set based on the method of least squares, under the constraint imposed by the conservation of energy Eqs. (11) and (14). Because the p-V equation [Eq. (13*b*)] consists of two equations, one for the high-pressure region and the other for the low-pressure region, and also because algebraic equations resulting from the application of the method of least squares are nonlinear, a computational program is developed to find the five unknowns. The program requires a set of initial guess values for the five unknowns. The parameters Λ, p_0, ΔV, V_U, of the error function p-V equation Eq. (1*b*) are used for initial values with the initial value for the fifth unknown $\hat{y}_{T0}$ being set to zero. The program employs the Newton-Raphson iterative

Table 1 Summary of inflation data analyses. 1. Obtained by applying the method of least squares along with error function *p-V* equation. 2. Results from the mechanistic model.

Data No.	Λ	p_0 [cmH_2O]	ΔV [L]	V_L [L]	$\hat{y}_{T0}$
A.1.	2.9652	22.398	2.3726	−0.0709	
2.	2.9578	22.411	2.3772	−0.0723	0.347
B.1.	2.7173	21.981	1.5612	−0.0762	
2.	2.7304	21.999	1.5559	−0.0728	0.359
C.1.	3.3532	25.082	1.6193	−0.0365	
2.	3.3664	25.073	1.6139	−0.0342	0.329
D.1.	1.6273	13.324	3.1567	−0.5727	
2.	1.9257	13.999	2.8392	−0.3542	0.379
E.1.	2.7160	30.361	1.6216	−0.0768	
2.	2.6497	30.817	1.6847	−0.0923	0.480
F.1.	2.6029	23.880	1.5066	−0.0962	
2.	2.6423	23.863	1.4874	−0.0873	0.365
G.1.	1.7288	20.156	3.0989	−0.3645	
2.	1.9277	20.731	2.8704	−0.2138	0.447
H.1.	1.8901	14.959	1.7905	−0.2185	
2.	2.0421	15.405	1.7129	−0.1563	0.431
I.1.	3.5379	25.248	2.7570	−0.0350	
2.	3.5449	25.232	2.7508	−0.0333	0.368
J.1.	2.7981	26.208	3.7326	−0.1583	
2.	2.7364	26.830	3.9129	−0.1887	0.474
K.1.	2.4296	17.895	1.3424	−0.0997	
2.	2.4708	17.951	1.3304	−0.0916	0.440
L.1.	1.2500	11.592	1.2470	−0.2829	
2.	1.5318	13.213	1.1256	−0.1678	0.695
M.1.	3.2725	29.865	3.9075	−0.0861	
2.	2.9972	30.327	4.2463	−0.2179	0.626
N.1.	2.7915	15.310	1.6284	−0.0705	
2.	2.8046	15.297	1.6219	−0.0681	0.358
O.1.	1.9487	18.374	1.8797	−0.2423	
2.	2.1412	18.837	1.7753	−0.1696	0.389
P.1.	2.4566	26.982	1.3277	−0.0787	
2.	2.4553	27.032	1.3278	−0.0773	0.467
Q.1.	2.1027	19.314	1.3316	−0.1279	
2.	2.2041	19.583	1.2941	−0.1004	0.389
R.1.	1.1672	13.986	2.0685	−0.5149	
2.	1.6209	16.352	1.7396	−0.2530	0.406
S.1.	3.1381	26.802	3.1306	−0.0851	
2.	3.0894	26.925	3.1878	−0.1030	0.407
T.1.	5.4709	30.038	1.7695	−0.0097	
2.	5.4708	30.037	1.7694	−0.0097	0.289
U.1.	3.2818	24.439	2.8956	−0.2075	
2.	3.2819	24.349	2.8956	−0.2075	0.327

technique around the value of $\hat{y}_{T0}$ to minimize the errors between Eq. (13*b*) and the data points, while the conservation of energy is satisfied exactly, until the five unknowns converge to a set of solutions. Various parameters obtained from the mechanistic model described above are summarized in Table 1.

5 Results and Discussion

We begin with physical interpretations of parameters of *p-V* equations in terms of the mechanistic model, represented by Eq. (12). The first equation in Eq. (12) is

$$\Delta V = N\hat{V}_0(\hat{y}_{T0} + 1)[=N(\hat{V}_0 + A_s\hat{y}_T)],$$

where $\hat{V}_0$ is the elemental volume increase due to alveolar opening and $A_s\hat{y}_T$ is the maximum elemental volume change due to elastic wall distension, represented by the upper limit of the volumetric piston displacement after alveolar opening. Therefore, ΔV (volume change between the two asymptotes, V_U and V_L) of the error function *p-V* equation is identified with a sum over all basic elements of the maximum volume available for inflation. Under the two-region *p-V* equation of the mechanistic model, the definition of ΔV needs to be elaborated. Since $V_L \neq V$ $(p \rightarrow -\infty)$ in the lower pressure solution, ΔV of the mechanistic model should be interpreted as the maximum possible volume change when the high pressure solution is extended into the low pressure region. However, the error minimization, applied between data points and the two region *p-V* equation makes it a good approximation to define ΔV as an overall volume change available for the inflation process. The second equation in Eq. (12), $p_0=(k/A_s)\hat{y}_0$, indicates that the pressure at the midpoint of the *p-V* curve is an equivalent pressure required to displace the piston against the spring force over the pop-open displacement of $\hat{y}_0$. It may be rewritten as $p_0\hat{V}_0=k\hat{y}_0^2$; therefore, $p_0\hat{V}_0/2$ is the spring energy required to displace the piston by the amount $\hat{y}_0$. This observation implies that the pressure p_0 is related to both the alveolar recruitment (through $\hat{y}_0$) and the elastic tissue distension (through k). A higher magnitude of p_0 may result from both a larger value of the spring constant (wall elasticity) and a greater amount of energy required to pop open the elements. The nondimensional parameter Λ is related to the parameter C of the mechanistic model through the third equation in Eq. (12), $C=(\sqrt{\pi}/4)\Lambda$. As may be seen from Eq.

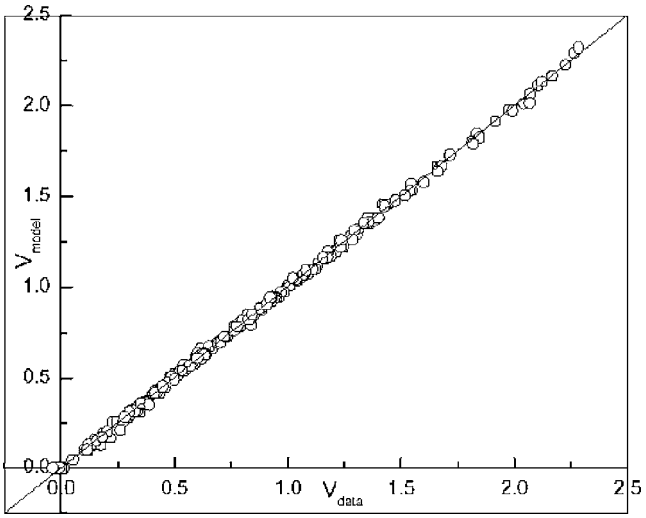

Fig. 4 *V* (volume predicted by model-based *p-V* equation) vs *V* (volume of data) for a specified pressure

(9), the parameter C appears as a factor in the function $I_3(p)$. Since $I_3(p)$ is a monotonically increasing function of p, an increase in volume V becomes more sensitive to a change in pressure when the magnitude of Λ is larger. The interpretations above may be further extended in terms of the distribution of elements over the critical pop-open pressure Eq. (13*c*). The number distribution of elements is a normal distribution with its mean at $\bar{p}(=p/p_0-1)$ and a standard deviation σ, which is proportional to $1/\Lambda$. Since the peak of the distribution is located at $\hat{p}_{cj}=\bar{p}$, the rate of increase in the number of open elements increases (decreases) for $p<p_0$ ($p>p_0$); an observation consistent with the fact that p_0 is a pressure at the inflection point of the error function *p-V* equation. A larger value of Λ indicates a smaller standard deviation, indicating a higher peak in number density and a sharper distribution; which is consistent with the observation on the *p-V* equation [Eq. (9)] that the volume change along a *p-V* curve becomes more responsive to the pressure change as Λ increases.

The *p-V* equation Eq. (13*b*) has three pressure-dependent terms. A term proportional to $\bar{p}$ in the equation for the low-pressure region (the third term) is due to elastic wall distension of nonalveolar elements (that is, due to piston displacement of elements that are open at $p=0$). Two other pressure-dependent functions are $I_2(\bar{p})$, originating from volume changes due to the piston displacement, and $I_3(\bar{p})$ which results from both the pop-open volume and the piston displacement. The former is symmetric with respect to $\bar{p}(=p/p_0-1)=0$, i.e., $I_2(\bar{p})=I_2(-\bar{p})$; while, the latter is antisymmetric, i.e., $I_3(\bar{p})=-I_3(-\bar{p})$. The *p-V* equation in the high pressure region $V(p_0\cdot\hat{y}_{T0}\leqslant p)$ is independent of the magnitude of $\hat{y}_{T0}$; while, the solution V_p [Eq. (13*a*)] is sensitive to the magnitude of $\hat{y}_{T0}$ in both the low- and high-pressure regions. Figure 4 is a plot of [the volume predicted by model-based *p-V* equation at a specified pressure] versus [the corresponding data volume] for all inflation data points from the twenty one data sets, showing good agreements between the model and the clinical data with $R^2=0.9993$.

Table 1 summarizes our analyses of the inflation data sets of patients with ARDS, based on the error-function *p-V* model equation as well as on the mechanistic model. Ranges of various parameters listed in Table 1 are

$$\Lambda = 1.5-5.5, \quad p_0 = 13-31\ [\mathrm{cmH_2O}], \quad \Delta V = 1-4\ [L],$$
$$\hat{y}_{T0} = 0.289-0.695.$$

The range of $\hat{y}_{T0}$ obtained by the mechanistic model indicates that

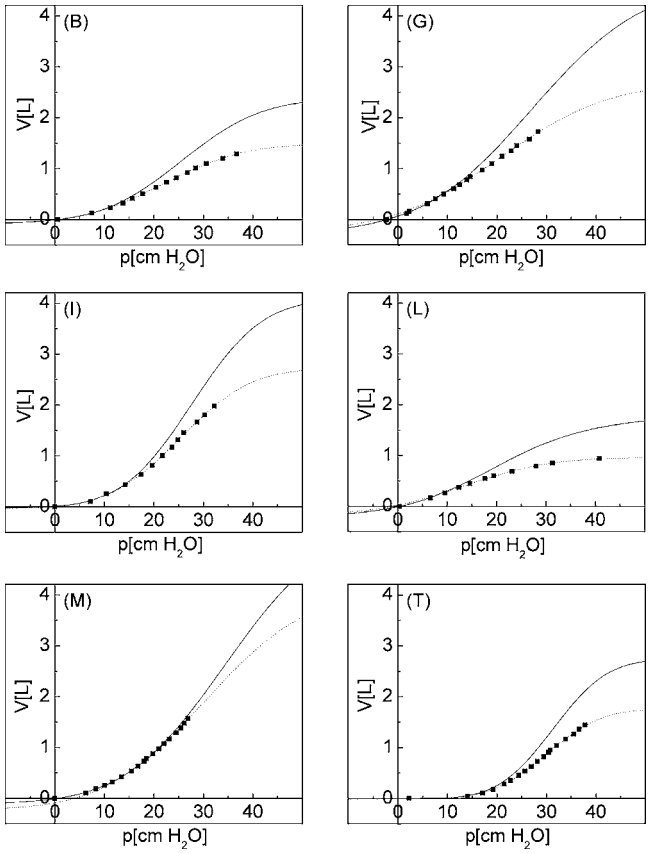

Fig. 5 Model-based *p-V* equation, Eq. (13*b*), vs data points for inflation process. Solid: solution for low-pressure region; dotted: solution for high-pressure region.

the fraction of total volume available for the pop-open mechanism (alveolar recruitment) $N\hat{V}_0/\Delta V$, which is equal to $1/(1+\hat{y}_{T0})$, ranges between 0.59 and 0.78. Since the boundary pressure between the low- and high-pressure solution, $p_0\cdot\hat{y}_{T0}$, is low compared to the end-of inflation pressure, the antisymmetric high-pressure solution is applicable over a major part of the measured pressure range of the data sets analyzed.

In addition to p_0 [inflection pressure where the first derivative (compliance) changes its sign], there are two important pressure indicators along the continuous *p-V* model equations; p_{mci} (pressure at the maximum compliance increase) and p_{mcd} (pressure at the maximum compliance decrease), where the third derivative is zero

$$\frac{p_{\mathrm{mcd}(i)}}{p_0} = 1 + (-)\frac{1.596}{\Lambda}. \tag{15}$$

The two pressure indicators p_{mci} and p_{mcd} correspond, respectively, to LIP and UIP of piecewise continuous *p-V* model equations. The mechanistic model yields another pressure indicator $p_0\hat{y}_{T0}$ as the boundary pressure between the high-pressure region and the low-pressure region.

Figure 5 shows six representative data sets of patients with ARDS as well as the corresponding *p-V* equation Eq. (13*b*). The solid (dotted) curves in Fig. 5 are the solution of the low (high) pressure region [i.e., the first (second) equation in Eq. (13*b*)] with the composite solution indicating that the *p-V* curve is not antisymmetric with respect to p_0. However, since the error minimization is applied between the antisymmetric error function *p-V* equation Eq. (1*b*) and the mechanistic model equation Eq. (13*b*) the two curves are very close to each other in the low pressure region of $0\leqslant p\leqslant p_0\hat{y}_{T0}$. Additional parameters of the mechanistic

model are listed below for the six data sets shown in Fig. 5 with pressure in [cmH_2O] and volume in [L].

Data	B	G	I	L	M	T
$N\hat{V}_0$	1.144	1.983	2.010	0.664	2.611	1.372
$N\hat{V}_0/\Delta V$	0.736	0.691	0.731	0.590	0.615	0.776
$p_0\hat{y}_{T0}$	7.897	9.266	9.285	9.183	18.984	8.680
p_{mci}	9.139	3.567	13.871	–	14.177	21.274
p_{mcd}/p_0	1.585	1.828	1.450	2.042	1.533	1.292

$N\hat{V}_0(=\Delta V/(1+\hat{y}_{T0}))$ is the total volume available for recruitment (through the pop-open mechanism); while $N\hat{V}_0/\Delta V$ represents $N\hat{V}_0$ as a fraction of total volume available for inflation (ΔV). Data B and I exhibit a similar fraction at ~73% although the actual volume available for recruitment is different between the two data sets. Similar observations (same fraction, different absolute values) may be made between Data L and M. A high value of the fraction (a low $\hat{y}_{T0}$ value) may be associated with the possibility of overdistension of wall tissues as recruited elements are saturated more easily. A comparison between the two pressure indicators $p_0\hat{y}_{T0}$ and p_{mci} in the table above demonstrates that the pressure at the maximum compliance increase may be located either in the low pressure region [Data G, and M with no p_{mci} (negative p_{mci}) for Data L] or in the high-pressure region [Data B, I, and T]. In the former case, all open elements are active (unsaturated) at $p=p_{\mathrm{mci}}$; in the latter case, however, the volume change at $p=p_{\mathrm{mci}}$ are affected by an increase in the number of saturated elements as both unsaturated and saturated elements are present in the high-pressure region. The pressure ratio p_{mcd}/p_0, shown in the last row of the table above also varies widely among the data sets. Equation (15) indicates that the pressure ratio depends on a single parameter Λ; hence, a pressure difference between p_{mcd} and p_0 as a fraction of the magnitude of p_0 $(p_{\mathrm{mcd}}-p_0)/p_0$ may be identified as the standard deviation σ of the distribution function Eq. (13*d*). In a data set with a large value of Λ the quasistatic volume change of TRS is more sensitive to the pressure change as p_{mcd} is located close to the inflection pressure with the corresponding elemental distribution showing a sharp distribution of elements over the critical pop-open pressure p_{cj}.

Although the present analysis is focused on the inflation process, there exist certain relations between the inflation and the deflation process that may be evaluated from the present inflation analyses. We consider a general case in which a quasistatic inflation process proceeds to a pressure, p_{ID} (end-of-inflation pressure=initial pressure of the corresponding deflation process), followed by a quasistatic deflation process. In terms of the mechanistic model, TRS elements at $p=p_{ID}$ with its critical pop-open pressure less than zero ($p_{cj}<0$) are still closed and have not contributed to the volume change during the inflation process from $p=0$ to $p=p_{ID}$; hence, we may postulate that only those elements that are open at $p=p_{ID}$ participate in the deflation process to follow. Therefore, V_U^d [an (imaginary) upper bound of volume for the deflation p-V curve] may be viewed as the volume which would be attained if the elements that are open at the end of the inflation process $p=p_{ID}$ were all fully saturated; i.e.,

$$V_U^d = V(p=p_{ID}) + N\hat{V}_0 \cdot \left[\int_0^{p_{ID}} (1+\hat{y}_{T0}) f(p=p_{ID}) dp_{cj} + \int_{p_{ID}}^{\infty} \hat{y}_{T0} \cdot f(p=p_{ID}) dp_{cj} \right] - V_p(p=p_{ID}). \quad (16a)$$

The first term on the right-hand side is the inflation volume at $p=p_{ID}$. The two integral terms together are the volume summed over all open elements at $p=p_{ID}$ when they are saturated, and the last term is the actual volume increase in the inflation process from $p=0$ to $p=p_{ID}$ with the last three terms representing a volume increase above $V(p=p_{ID})$ if all open elements at p_{ID} were saturated. Under the assumption that the magnitude of p_{ID} is greater than $B(\equiv p_0\hat{y}_{T0})$, which is valid for all data sets analyzed, Eq. (13*d*) is used to evaluate the right-hand side of Eq. (16*a*), yielding

$$V_U^d = V_L + \frac{2\Delta V}{\pi\Lambda(1+\hat{y}_{T0})} \cdot I_5 + \frac{\Delta V}{2} \cdot [1 + I_3(\bar{p}_{ID})] + \frac{\Delta V(1-\hat{y}_{T0})}{2(1+\hat{y}_{T0})}(I_4 - I_1). \quad (16b)$$

The clinical data sets contain both the inflation and the deflation p-V curves for each patient with ARDS; however, the p-V curves are obtained separately for the inflation and the deflation process. (See [2] for the procedure of data acquisition.) Figure 6 shows inflation (unfilled) and deflation (filled) data points, as well as the corresponding inflation (I) and deflation (D) curves for a typical data set we examined. The inflation curve in Fig. 6 is Eq. (13) of the mechanistic model; while, the deflation curve is obtained by the method of least squares applied between data points and the error function p-V equation Eq. (1). As shown in Fig. 6, the end-of-inflation point is different from the initial deflation point for most data sets. To accommodate the data into the analysis based on Eq. (16*b*), the initial deflation data point is translated horizontally until it meets the inflation p-V curve, the pressure value of which is then defined as p_{ID} in Eq. (16*b*). (See Fig. 6.) This implies that the deflation curve preceded by an inflation curve is assumed to be the same as the deflation curve of data sets horizontally translated until the beginning-of-deflation data point is on the inflation curve.

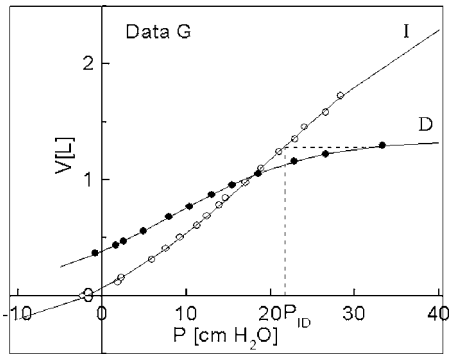

Fig. 6 Data points for inflation (unfilled) and deflation (filled). *p-V* equation of mechanistic model for inflation (*I*) and the error function *p-V* equation for deflation (*D*).

Figure 7 presents V_U^d of Eq. (16*b*), predicted from the mechanistic model of the inflation process, plotted against V_U^d of the error-function p-V equation. (For a list of numerical results relevant to the analysis, see Table 2.) A maximum and a minimum of a difference, V_U^d [Eq. (16*b*)]—V_U^d [Eq. (1*b*)], are 0.1113 [L] and −0.0352 [L], respectively, with an average of the difference =0.0460 [L]. Agreements are very good in view of the fact that Eq. (16*b*) predicts the upper volume asymptote of the deflation process in terms of the conditions predicted by the mechanistic model for the corresponding inflation process; thus indirectly supporting a certain degree of validity of the mechanistic model. Also, the fact that the magnitude of p_{ID} is determined from the horizontal translation of the deflation curve indicates that the magnitude of V_U^d may be relatively insensitive to the inflation history prior to $p=p_{ID}$. On the other hand, a closer examination of Fig. 7 indicates that the mechanistic model slightly underpredicts V_U^d compared to that of the error-function equation for most of data sets. This could be interpreted as the effects of the horizontal shift

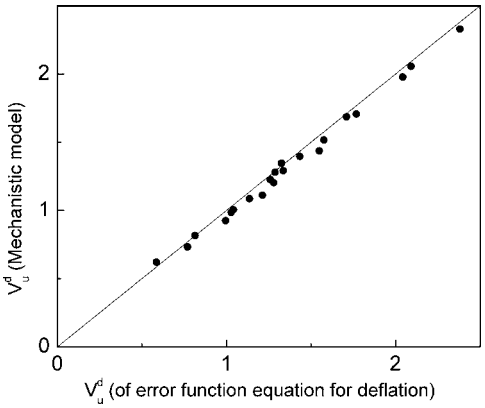

Fig. 7 V_U^d (predicted from the mechanistic model) vs V_U^d (of error-function p-V equation for deflation)

of the deflation curve. Equation (16*b*) for V_U^d contains p_{ID} as a variable for specified inflation conditions, demonstrating that the magnitude of V_U^d (which affects the shape of the deflation curve) depends on the end-of-inflation pressure.

6 Summary and Conclusions

A mechanistic model of TRS elements, each consisting of a piston-spring system, is developed to analyze quasistatic pressure-volume curves for the inflation process. The model accommodates both the alveolar recruitment (in terms of the critical pop-open pressure) and the elastic distension of wall tissues (in terms of the piston displacement). The Boltzmann statistical probability yields the distribution of a large population of the basic elements in TRS with the critical pop-open pressure as the distribution parameter. Under the constraint imposed by the conservation of energy, the parameters of the model-based p-V equation are determined for each clinical data set by a computational error minimization procedure. The p-V equation thus derived Eq. (13*b*) consists of two equations; one for the low-pressure region where all open elements are active (=unsaturated) as the piston of an element is yet to reach its stroke limit, and the other for the high-pressure region where some open elements are saturated. The elemental distribution over the critical pop-open pressure Eq. (13*c*) is a normal distribution with its shape (the mean and the standard deviation) affected substantially by the magnitudes of two parameters in the p-V equation Λ and p_0. A good agreement between model-predicted V_U^d and the data-based V_U^d in Fig. 7 serves as a validity of the proposed mechanistic model. Equation (12) gives relations

Table 2 Summary of deflation data analyses. 1. Obtained by method of least squares with error function p-V equation for deflation process. 2. Predictions from the mechanistic model of inflation process.

Data No.	Λ^d	p_0^d [cmH_2O]	ΔV^d [L]	V_L^d [L]	V_U^d [L]
A 1.	1.4712	11.410	1.9214	−0.1528	1.7685
2.					1.7064
B 1.	1.5528	12.975	1.4115	−0.1227	1.2887
2.					1.2808
C 1.	2.1564	15.828	1.2352	0.0297	1.2599
2.					1.2259
D 1.	1.0772	6.846	2.7012	−0.6096	2.0915
2.					2.0572
E 1.	2.2044	15.602	0.7009	0.0703	0.7712
2.					0.7329
F 1.	1.7995	14.418	1.0476	−0.0527	0.9948
2.					0.9252
G 1.	0.9839	8.140	1.2811	0.0454	1.3265
2.					1.3455
H 1.	0.7147	6.472	2.0772	−1.0349	1.0423
2.					1.0053
I 1.	2.1010	14.157	1.4798	0.5637	2.0435
2.					1.9784
J 1.	1.6600	13.404	1.8960	0.028	1.7103
2.					1.6858
K 1.	1.0577	9.778	1.5070	−0.3657	1.1412
2.					1.0860
L 1.	0.3107	3.151	1.3930	−0.8076	0.5853
2.					0.6206
M 1.	2.1702	14.989	1.4322	0.1442	1.5764
2.					1.5163
N 1.	0.7220	6.45	2.4020	−1.1900	1.2140
2.					1.1115
O 1.	1.0558	10.969	1.8684	−0.3195	1.5488
2.					1.4375
P 1.	1.5406	12.231	0.7461	0.0684	0.8145
2.					0.8154
Q 1.	1.1691	10.670	1.1801	−0.1515	1.0285
2.					0.9857
R 1.	0.8643	8.1411	1.8260	−0.4893	1.3366
2.					1.2923
S 1.	2.7458	17.050	2.0015	−0.5673	1.4341
2.					1.3962
T 1.	4.5056	23.619	1.1748	0.1057	1.2805
2.					1.2026
U 1.	2.9735	18.599	2.3404	0.0408	2.3812
2.					2.3305

between the parameters in the error function p-V equation Eqs. (1a) and (1b), and the parameters of the mechanistic model.

Since we have two equations [the first two equations in Eq. (12)] with four unknown parameters [N, $\hat{V}_0$ (or $\hat{y}_0$, k, A_s] of the basic elements, additional quantitative information other than the parameters of the p-V equation, would be required if one tries to determine the magnitudes of these four parameters. Also the proposed model is constructed from a simplified basic element as the heterogeneity in elemental properties, for example, is not taken into account. Despite these limitations, the present model recovers the error-function p-V equation as the p-V equation of the high-pressure region ($p \geqslant p_0 \hat{y}_{T0}$), which covers a major part of the pressure range along p-V curves. There are three parameters associated with the piecewise continuous p-V model equation, (chord) compliance of the linear midregion, LIP and UIP. In the continuous p-V model equation, the local compliance (dV/dp) changes continuously with its maximum at the inflection pressure p_0. LIP and UIP are, respectively, replaced by p_{mci} and p_{mcd}. The mechanistic model identifies p_0, Λ and $\hat{y}_{T0}$ as the three independent parameters that are absent in the piecewise continuous p-V model equation. These parameters characterize differences among p-V curves and their distribution functions as p_{mci}, p_{mcd} as well as the local compliance are dependent on the magnitude of these parameters. Harris et al. [2] through clinical trials demonstrated advantages of the continuous p-V model equation over the piecewise continuous equation for clinical applications. The present report may be viewed as a theoretical justification and basis for the use of the continuous p-V model equation.

Acknowledgments

We are grateful to Dr. S. R. Harris and Dr. J. G. Venegas at Massachusetts General Hospital for making the p-V data available to us. The U.S. Army Medical Research and Materiel Command under DAMD17-02-1-0915 supported this work.

Nomenclature

A = $(k/A_s)\hat{y}_0 = p_0$

A_s = piston surface area on which pressure is acting (Fig. 4)

B = $(k/A_s)\hat{y}_T = p_0 \cdot \hat{y}_{T0}$, threshold pressure for onset of saturation

C = $(\hat{\beta}/2)^{1/2} \cdot p_0 = \sqrt{\pi}\Lambda/4$

f, F = distribution functions [Eqs. (6) and (13c)]

I_1 = $\mathrm{erf}(C)$, defined in Eq. (13b)

I_2 = $\exp(-C^2\bar{p}^2) - \exp(-C^2)$, defined in Eq. (13$b$)

I_3 = $\mathrm{erf}(C\bar{p})$, defined in Eq. (13b)

I_4 = $\mathrm{erf}[C(1-\hat{y_{T0}})]$, defined in Eq. (13$b$)

I_5 = $\exp[-C^2(\hat{y}_{T0}-1)^2] - \exp(-C^2)$, defined in Eq. (13$b$)

k = spring constant [N/m] (Fig. 4)

N = total number of TRS elements

N_j = number of elements at energy level j

p = pressure (interpleural pressure difference)

$\bar{p}$ = nondimensional pressure, $p/p_0 - 1$

p_{cj} = critical pressure at which an element j, "pops open"

$\hat{p}_{cj}$ = p_{cj}/p_0 [Eq. (13c)]

p_f = pressure at the end of inflation process

p_{ID} = pressure at the intersect of inflation and deflation processes

$p_{\mathrm{mci}(d)}$ = pressure at maximum compliance increase (decrease)

p_0 = pressure at the inflection point in p-V equation, Eq. (1)

$U(p)$ = total energy of TRS at $p = p$

ΔU = $\equiv U(p=p_f) - U(p=0)$

V = volume

V_p = volume change from the state of $p=0$

$V_{L(U)}$ = lower (upper) volume asymptote (Fig. 1)

V_U^d = an (imaginary) upper bound of volume for the deflation process

$\bar{V}$ = nondimensional volume, $V - [(V_U + V_L)/2]/(\Delta V/2)$, [Eq. (2)]

$\hat{V}_j$ = volume of an element j

ΔV = $V_U - V_L = N\hat{V}_0(\hat{y}_{T0}+1)$

$\hat{V}_0$ = "pop-open" volume ($=A_s\hat{y}_0$) (Fig. 4)

$\hat{y}_j$ = piston displacement of an element j (Fig. 4)

$\hat{y}_0$ = "pop-open" displacement, ($=\hat{V}_0/A_s$) (Fig. 4)

$\hat{y}_T$ = piston stroke limit (Fig. 4)

$\hat{y}_{T0}$ = $\hat{y}_T/\hat{y}_0$

Greek symbols

α = constant of proportionality [Eq. (1a)]

β = constant in the distribution function [Eq. (4)]

$\hat{\beta}$ = $(A_s^2/k)\beta$ [Eq. (5)]

$\hat{\epsilon}_j$ = energy stored in an element j [Eq. (3)]

$\hat{\epsilon}_{jA}$ = elemental activation (pop-open) energy

$\hat{\epsilon}_{jS}$ = elemental energy due to spring displacement

Λ = $\alpha p_0 \Delta V$ (nondimensional parameter) [Eq. (1)]

σ = $(8/\pi)^{1/2}/\Lambda$, the standard deviation [Eq. (13c)]

ω = $\Lambda\bar{p}/2$ [Eq. (2)]

Acronyms

ARDS = acute respiratory distress syndrome

LIP = lower inflection point

mcd(i) = maximum compliance decrease (increase)

TRS = total respiratory system

UIP = upper inflection point

References

[1] Venegas, J. G., Harris, S. R., and Simon, B. A., 1998, "A Comprehensive Equation for the Pulmonary Pressure-Volume Curve," J. Appl. Phys., **84**(1), pp. 389–395.

[2] Harris, S. R., Hess, D. R., and Venegas, J. G., 2000, "An Objective Analysis of the Pressure-Volume Curve in the Acute Respiratory Distress Syndrome," Am. J. Respir. Crit. Care Med., **161**, pp. 432–439.

[3] Jonson, B., and Svantesson, C., 1999, "Elastic Pressure-Volume Curves: What Information Do They Convey?," Thorax, **54**, pp. 82–87.

[4] Amato, M. B., Barbas, C. S., Medeiros, D. M., Schettino, G. D. P., Lorenzi, F. G., Kairalla, R. A., Deheinzelin, D., Morais, C., Fernandes, E. D. O., and Takagaki, T. Y., 1995, "Beneficial Effects of the "Open Lung Approach" with Low Distending Pressures in Acute Respiratory Distress Syndrome. A Prospective Randomized Study on Mechanical Ventilation," Am. J. Respir. Crit. Care Med., **152**, pp. 1835–1846.

[5] Amato, M. B., Barbas, C. S., Medeiros, D. M., Magaldi, G. P., Schettino, G. D. P., Kairalla, R. A., Deheinzelin, D., Munozs, C., Oliveira, R., Takagaki, T. Y., and Calvalho, C. R., 1998, "Effect of a Protective-Ventilation Strategy on Mortality in the Acute Respiratory Distress Syndrome," N. Engl. J. Med., **338**(6), pp. 347–354.

[6] ARDS Network, 2000, "Ventilation with Lower Tidal Volumes as Compared with Traditional Tidal Volumes for Acute Lung Injury and the Acute Respiratory Distress Syndrome," N. Engl. J. Med., **342**(18), pp. 1301–1308.

[7] Salazar, E., and Knowles, J. H., 1964, "An Analysis of Pressure-Volume Characteristics of the Lungs," J. Appl. Physiol., **19**, pp. 97–104.

[8] Paiva, M., Yernault, J. C., VanErdeweghe, P., and Englert, M., 1975, "A Sigmoidal Model of the Static Volume-Pressure Curve of Human Lung," Respir. Physiol., **23**, pp. 317–323.

[9] Murphy, B. G., and Engel, L. A., 1978, "Models of the Pressure-Volume Relationship of the Human Lung," Respir. Physiol., **32**, pp. 183–194.

[10] Gibson, G. J., Pride, J. B., Davis, J., and Schroter, R. C., 1979, "Exponential

Description of the Static Pressure-Volume Curve of Normal and Diseased Lungs," Am. Rev. Respir. Dis., **120**, pp. 799–811.
[11] Bogaard, J. M., Overbeek, S. E., Verbraak, A. F., Vons, C., Folgering, H. T., Van, D. M. T. C., Roos, M., and Sterk, P. J., 1995, "Pressure-Volume Analysis of the Lung with an Exponential and Linear-Exponential Model in Asthma and COPD," Eur. Respir. J., **8**, pp. 1525–1531.
[12] Svantesson, C., Sigurdsson, S., Larsson, A., and Jonson, B., 1998, "Effects of Recruitment of Collapsed Lung Units on Elastic Pressure-Volume Relationship in Anaesthetized Healthy Adults," Acta Anaesthesiol. Scand., **42**, pp. 721–728.
[13] Hickling, K. G., 1998, "The Pressure-Volume Curve is Greatly Modified by Recruitment. A Mathematical Model of ARDS Lungs," Am. J. Respir. Crit. Care Med., **158**, pp. 194–202.
[14] Narusawa, U., 2001, "General Characteristics of the Sigmoidal Model Equation Representing Quasi-Static Pulmonary Pressure-Volume Curves," J. Appl. Physiol., **91**, pp. 201–210.
[15] Sonntag, R. E., and Van Wylen, G. J., 1966, *Fundamentals of Statistical Thermodynamics*, Wiley, New York.
[16] Fowler, R., and Guggenheim, E. A., 1956, *Statistical Thermodynamics*, Cambridge University Press, Cambridge, England.